

Deep drilling of silica glass by continuous-wave laser backside irradiation

Hirofumi Hidai¹ · Namiko Saito¹ · Souta Matsusaka¹ · Akira Chiba¹ · Noboru Morita¹

Received: 24 July 2015 / Accepted: 19 October 2015 / Published online: 7 March 2016
© Springer-Verlag Berlin Heidelberg 2016

Abstract We propose a novel method for drilling of silica glass based on the continuous-wave laser backside irradiation (CW-LBI) phenomenon. The method allows drilling to be performed by single-shot irradiation using a CW laser. A spindle-shaped emission is generated in the bulk glass and is then guided to the glass surface, and at the instant that the beam reaches the surface, the glass material is ejected. The glass ejection process occurs for a time of $\sim 250 \mu\text{s}$. A hole that is similar in shape to that of the spindle-shaped emission is left. The hole length tended to increase linearly with increasing laser power. The laser power dependence of the spindle-shaped emission propagation velocity is also linear, and the velocity increases with increasing laser power. The hole diameters were smaller in the case where the laser focus position was set on the glass surface, and these diameters increased with increasing defocusing. The maximum hole depth reached more than 5 mm. Through-hole drilling was demonstrated using a 3-mm-thick glass substrate.

1 Introduction

Glass has commonly been used in optical devices and microfluidics because of its transparency and chemical resistance. In the case of glass drilling [1], percussion drilling using ultrafast lasers [2–5], ultraviolet nanosecond lasers [6, 7] and microsecond CO₂ lasers [8] has been reported. In addition, the transparency property of glass has

been used. High-aspect-ratio drilling where the process has been initiated from backside illumination rather than from a laser-irradiated front surface has been reported in the literature [9, 10]. In these previous studies, pulse lasers with high peak power have been used. Irradiation with a high-power pulsed laser leads to ablation of the material in the vicinity of the surface. Each pulse ablates the material slightly, and deeper holes are processed by repetitive illumination in percussion drilling.

A phenomenon called fiber fuse has been described in the literature [11–13]. When a fiber fuse occurs in an optical fiber, the fiber is damaged. Fiber fuses are initiated on an edge face or at a material defect when a high-power density laser is used to illuminate the fiber. The initiation point temperature is elevated, and then, the glass begins to absorb the light [13]. This light absorption induces an additional increase in temperature, and the high-temperature region eventually becomes luminous plasma. The emission then migrates toward the light source supplying the illumination [12]. The emission temperature is estimated to reach the 5000–10,000 K range [11]. This high temperature then causes SiO₂ degradation, which produces SiO and O₂, and the O₂ gas forms voids in the fiber [13, 14].

The authors have found that a similar phenomenon occurs in bulk glass and have named this phenomenon continuous-wave laser backside irradiation (CW-LBI) [15–17]. An absorbent is first placed on one of the bulk glass surfaces. When a continuous-wave (CW) laser irradiates this absorbent from the glass side, i.e., through the glass, the CW-LBI phenomenon, which is essentially the same as the fiber fuse phenomenon, is induced in the glass. Clarification of the process [15], evaluation of the resulting modification [16] and process temperature calculations [17] have been reported previously.

✉ Hirofumi Hidai
hidai@faculty.chiba-u.jp

¹ Department of Mechanical Engineering, Chiba University,
1-33 Yayoi-cho, Inage-ku, Chiba 263-8522, Japan

We propose herein the following novel method of glass drilling using a CW laser. In laser drilling, repetitive irradiation of a surface with high-peak-power laser pulses has been used and the process progresses on the surface as described above. In contrast, our method permits one-step glass drilling via single-shot irradiation using a CW laser. Removal of the entire amount of material corresponding to a drilled hole occurs in a single step. In the fiber fuse and CW-LBI phenomena, a high-temperature and high-pressure plasma region moves within the material. When this plasma region is guided to the glass surface, the pressure is relieved as the glass material vaporizes; SiO₂ then degrades to produce SiO and O₂, and the softened glass is ejected. As a result, a hole that has the same shape as the plasma is drilled in the glass. In this paper, a hole with length of >5 mm was drilled in silica glass using the proposed method. Silica glass was used in this study because its thermal shock resistance is high and CW-LBI had been confirmed to occur in silica glass. A high-power laser was used as the light source to lengthen the plasma. In addition, the plasma behavior was observed with a high-speed camera, and the effects of both the laser power and the defocus distance on the drilled hole shape were clarified.

2 Experimental

Figure 1 shows the experimental setup, which was roughly the same as that used in our previous papers [15, 16]. A brief description of the setup is given as follows. A CW fiber laser (FLC-300-A, Fujikura, Ltd., Tokyo, Japan) with an oscillation wavelength of 1095 nm was used for the experiments. The beam profile was TEM₀₀ mode. The maximum laser power was 277 W. The laser beam, which was emitted from the oscillator with a diameter of 5.8 mm, was focused using a convex lens with a focal length of 407 mm.

The beam profile was estimated using the following equations [18]:

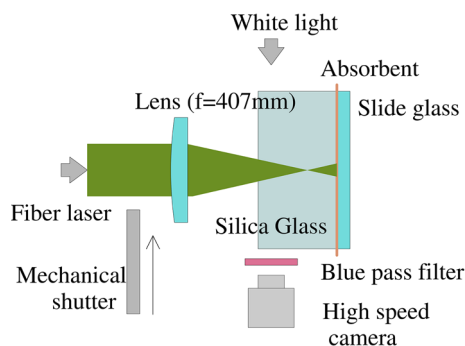


Fig. 1 Illustration of experimental setup

$$\omega_0 = \frac{2\lambda f}{\pi a}, \quad (1)$$

$$z_r = \frac{\pi\omega_0^2}{\lambda}, \quad (2)$$

$$\omega(z) = \omega_0 \left[1 + \left(\frac{z}{z_r} \right)^2 \right]^{1/2}, \quad (3)$$

$$I(r) = \frac{2P}{\pi\omega(z)^2} \exp\left(-\frac{2r^2}{\omega(z)^2}\right). \quad (4)$$

Here, ω_0 is the spot radius ($1/e^2$), λ is the wavelength, f is the focal length, a is the diameter of the laser beam emitted from the oscillator, z_r is the Rayleigh length, P is the total power, $\omega(z)$ is the beam radius at z , $I(r)$ is the laser density at r , z is the distance from the focal spot along the optical axis and r is the distance from the center of the focal spot. The calculated spot diameter at the focus was $\sim 100 \mu\text{m}$, and the Rayleigh range was 6.6 mm. A silica glass sample with a thickness of 10 mm, an absorbent layer and a slide glass were layered using a jig. A 10- μm -thick copper foil (CU-113173, Nilaco Corp., Tokyo, Japan) was used as the absorbent. To ensure good contact between the silica glass and the absorbent, a slide glass (S1111, Matsunami Glass Ind., Ltd. Osaka, Japan) was used. The focused beam was used to illuminate the absorbent through the silica glass. The defocus distance was defined as zero when the focus was matched on the laser oscillator side surface of the silica glass, and was defined as being positive when the distance between the glass sample and the lens was longer than the focal distance. The laser irradiation time was controlled using a mechanical shutter (SH05, Thorlabs Inc., Newton, NJ, USA) placed between the focusing lens and the laser oscillator. The shutter opening time was set at 0.5 s, and in the case where no hole was observed, the opening time was extended up to 1 s. However, the shutter opening time should be assumed to be 0.5 s unless otherwise stated.

A high-speed camera (Phantom V7.3, Vision Research, Inc., Wayne, NJ, USA) was set in an orthogonally crossed position relative to the laser beam axis. A high-speed movie was recorded with a frame rate of 20,000 frames per second, 512×256 resolution and an exposure time of 40 μs . Shadowgraphs were observed under backlit illumination. The bright plasma emission was filtered by placing a blue pass filter (10BPF10-440, Newport Corp., CA, USA) in front of the camera.

3 Results and discussion

Under laser illumination, a spindle-shaped emission moved toward the light source from the vicinity of the absorbent. When the forefront of the spindle-shaped emission reached

the silica glass surface, the glass was ejected from the surface with an explosive sound. A hole was thus drilled in the substrate, and modifications were left along the trajectory. To clarify and discuss this process in detail, this section has been divided into the following five subsections.

In Sect. 3.1, the results of in situ observation of the drilling process are shown. The laser irradiation side surface of the sample glass was observed with a high-speed camera, and the in situ observation clarified the various stages of the drilling process. In Sect. 3.2, the results of microscope observation of a processed substrate are shown. The shape of the drilled hole and the appearance of the modifications that were left after the process were clarified by observation of the entire emission trajectory. In Sect. 3.3, the effects of both the laser power and the laser beam diameter on the shape of the drilled hole are clarified. Changes in the laser power caused the hole and spindle-shaped emission lengths to vary, and the effects of the laser beam diameter on the drilled hole were investigated by varying the laser focus position. In addition, the beam intensity profile at the glass surface on the light source side was calculated to determine the laser intensity range where the glass became luminous. In Sect. 3.4, the drilling process is discussed with reference to the experimental results and to the results of previous papers. In Sect. 3.5, a through-hole drilling process is demonstrated. Two glass pieces were prepared. One was set on an absorbent and acted as an initiation glass. The other piece was set on the light source side surface of the initiation glass and acted as the workpiece. In the case where the workpiece is thinner than the maximum length of the drilled hole, through-hole drilling of the workpiece glass can be expected. The entire process was observed using the high-speed camera.

3.1 In situ observation

Figure 2 shows a typical in situ observation result for a laser power of 212 W and a defocus of -7 mm. The spindle-shaped emission length was ~ 3 mm, and the spindle-shaped emission propagation velocity was ~ 600 mm/s. The spindle-shaped emission movement caused rapid heating and quenching of the glass, and a modified zone was thus formed in the trajectory. The dark dots that were observed in the modification area (marked by circles in Fig. 2) were voids. The frame in which glass ejection was observed as a dark shadow shown on the left side of the silica glass was defined as 0 s. A dark shadow appeared around both the hole and the modification at the same instant as the ejection occurred, i.e., at 0 μ s. The dark shadow around the hole disappeared as time passed. At +20 ms, a hole with length of ~ 4 mm was formed. Note that the laser continued to provide illumination after the

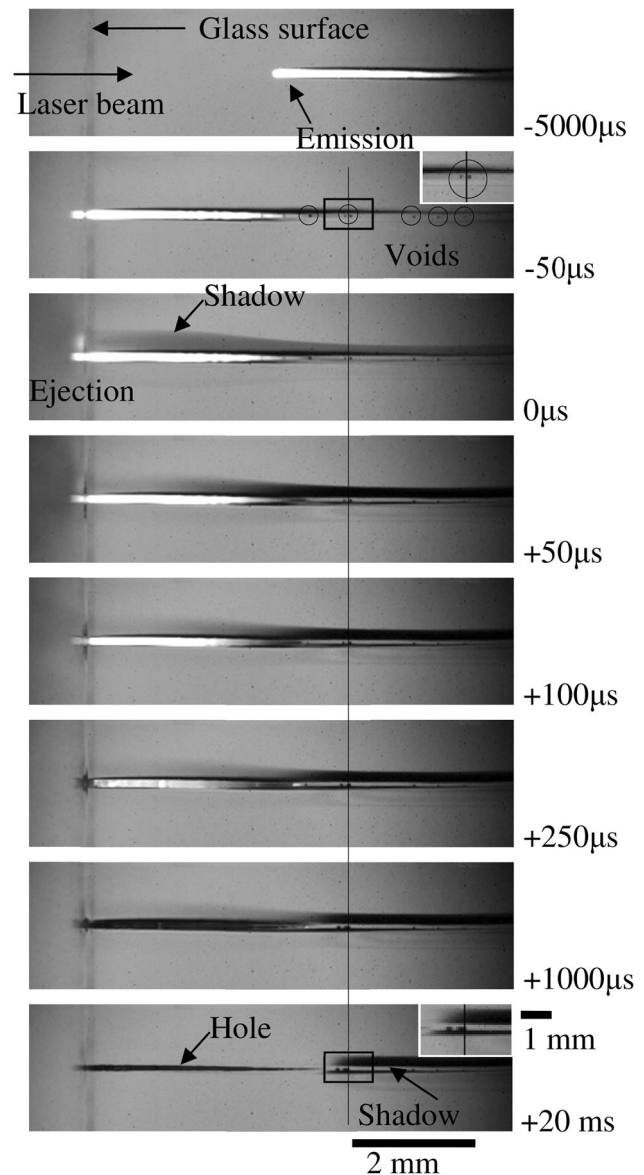


Fig. 2 Time-lapse photographs taken during emission propagation and hole formation. The laser power was 212 W, and the defocus distance was -7 mm. *Insets* show magnified images of the areas marked using *rectangles*

hole was formed. The glass was transparent to the laser beam, and thus, the profile of the hole did not change, even when the laser illumination time was increased, because the heated zone was eliminated by the ejection process and the glass does not absorb the laser beam. However, the laser illumination does heat the absorbent, and long-term illumination can cause it to crack.

In Fig. 2, a vertical line is drawn between the two voids that were observed at -50 μ s. The insets in the figure show magnified images of the two voids, which are marked using squares. The two voids were tracked with the intent of observing the glass flow at the bottom of the hole. No

transformation was detected during the period from -50 to 0 μs . At $+100$ μs , a small degree of void transfer was observed, and the right void overlapped the vertical line. The voids were transferred up to the time of $+1000$ μs . In addition, the two voids had also expanded. Consideration of the above phenomena indicated that the temperature in the material surrounding the voids was high as the glass flowed. This high temperature simultaneously caused high pressure. When the spindle-shaped emission reached the surface of the glass, the pressure was released. As a result, the voids expanded and the glass surrounding the voids flowed.

3.2 Microscopic observation

Figure 3 shows micrographs of the spindle-shaped emission trajectory. The left side of Fig. 3 is shown in Fig. 2. A spindle-shaped hole with a depth of ~ 4 mm was formed from the laser-illuminated side. The glass surface of the laser-illuminated side is defined as a reference depth of 0 mm. The hole diameter was ~ 90 μm at the glass surface. This diameter then increased with increasing hole depth, and the maximum diameter was ~ 110 μm in the depth range of 100 – 800 μm . The diameter then decreased with increasing hole depth in the area where the hole was deeper than 800 μm . Modifications were observed in the areas of the glass that were deeper than the bottom of the hole. Cracks were observed as dark shadows. Figure 3b shows a magnified image of the bottom of the hole, which is marked using a square in Fig. 3a. A double-layered structure is observed along the spindle-shaped emission trajectory.

3.3 Influence of laser illumination conditions on hole and spindle-shaped emission

Figure 4 shows the laser power dependence of the spindle-shaped emission and the hole length. Figure 4a–d shows

typical experimental results. Figure 4e shows the laser power dependence of the spindle-shaped emission lengths that were observed immediately before glass ejection and the hole lengths that were measured after the laser irradiation was terminated and sufficient time had passed. The spindle-shaped emission length was defined as the area over a specific brightness. The experiments were carried out three times under identical laser power conditions. No modifications were induced by laser powers of 89 W. The laser intensity herein refers to the average power density at the beam spot on the laser-illuminated side of the surface. Figure 4e shows that the spindle-shaped emission and hole lengths increase linearly with increasing laser power. The maximum hole length exceeded 5 mm. The diameters of the thickest parts of the spindle-shaped emission and the hole were 145 – 170 and 80 – 125 μm , respectively, and no clear dependence between the laser power and these diameters was observed. Figure 4f shows the laser power dependence of the averaged spindle-shaped emission propagation velocity. The spindle-shaped emission propagation velocity was obtained from the high-speed movie. Specifically, the positions of the spindle-shaped emission forefront at the moment that it reached the glass surface and at the point 5 ms before it reached the glass surface were used to calculate the velocity. Figure 4f shows that the laser power dependence of the spindle-shaped emission propagation velocity is also linear. The spindle-shaped emission propagation velocity was in the 350 – 750 m/s range. Figure 4g shows the relationships between the spindle-shaped emission propagation velocity and the hole and spindle-shaped emission lengths. Figure 4g shows that these relationships also maintain linearity.

The influence of the laser beam diameter on both the spindle-shaped emission and the hole is shown in Fig. 5. Figure 5a, b shows typical examples of observations of the spindle-shaped emission and the drilled hole, respectively, using a laser power of 212 W and a defocus distance of -37 mm. When compared with the spindle-shaped

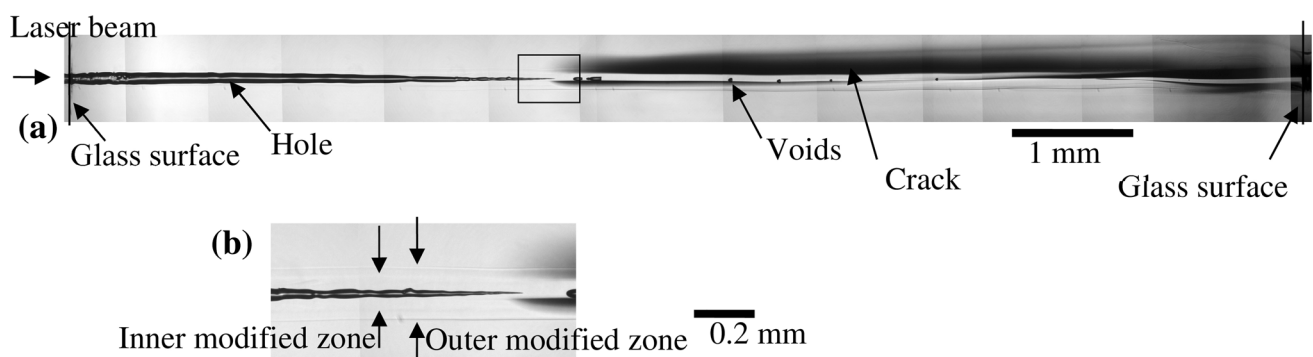


Fig. 3 Transverse cross section and profile of the drilled hole and the modified area. **b** A magnified image of the area marked using a square in **a**. The laser power was 212 W, and the defocus distance was -7 mm

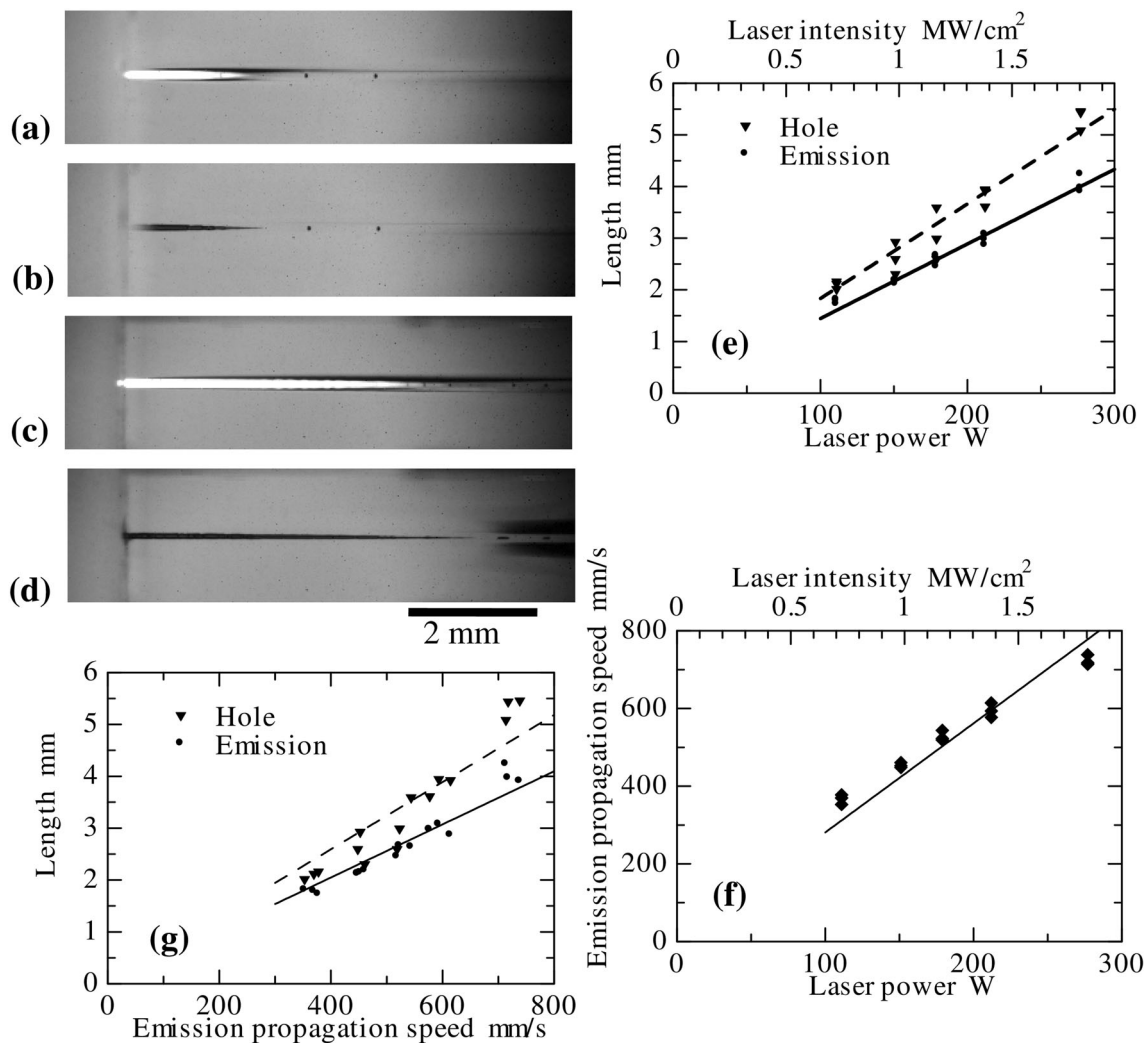


Fig. 4 Holes drilled using different laser powers. Snapshots taken one frame before the ejection are shown in **a** and **c**, and the transverse cross section and the profile of the drilled hole and the modified area in each case are shown in **b** and **d**. The laser power was 111 W in **a** and **b** and 277 W in **c** and **d**. **e** The influence of the laser power on

the lengths of both emission and hole. **f** The propagation velocity dependence on laser power. **g** The relationship between emission propagation velocity and the emission and hole lengths. The defocus distance was -7 mm. The illumination time was set at 0.7 s at 111 W and at 0.5 s at >151 W

emission at the defocus distance of -7 mm (Fig. 2), the spindle-shaped emission in this case was both shorter and thicker. Figure 5c shows the focus position dependence of the drilled hole and spindle-shaped emission diameters. These experiments were carried out three times using the same focus position and under the same conditions, in a similar manner to the power influence experiments performed earlier. The focus position was changed from -47 to 37 mm, and the CW-LBI phenomenon was not observed at the focus positions of 37 and -47 mm. The diameters of the holes and the spindle-shaped emissions varied with the changing focus positions. Both diameters were smaller at the focus position of ~ 0 mm, and both increased by defocusing. The diameters of the holes and the spindle-shaped emissions ranged from ~ 110 to ~ 220 μm and from ~ 150 to ~ 330 μm , respectively.

Figure 5d shows optical calculation results for the beam intensity profile at the glass surface on the light source side. The calculation conditions assumed that the laser light beam used for irradiation had a Gaussian distribution and was focused using a convex lens. Cross marks indicate the average values of the spindle-shaped emission radius, as shown in Fig. 5c. Figure 5d shows that the glass became luminous when the laser intensity was in the 900–2400 W/cm² range.

3.4 Discussion of drilling process

Figure 6 shows a schema of the drilling mechanism. Because the high-temperature region radiates light, the phenomenon where the spindle-shaped emission moves toward the light source is observed. In the light absorption zone, the glass can

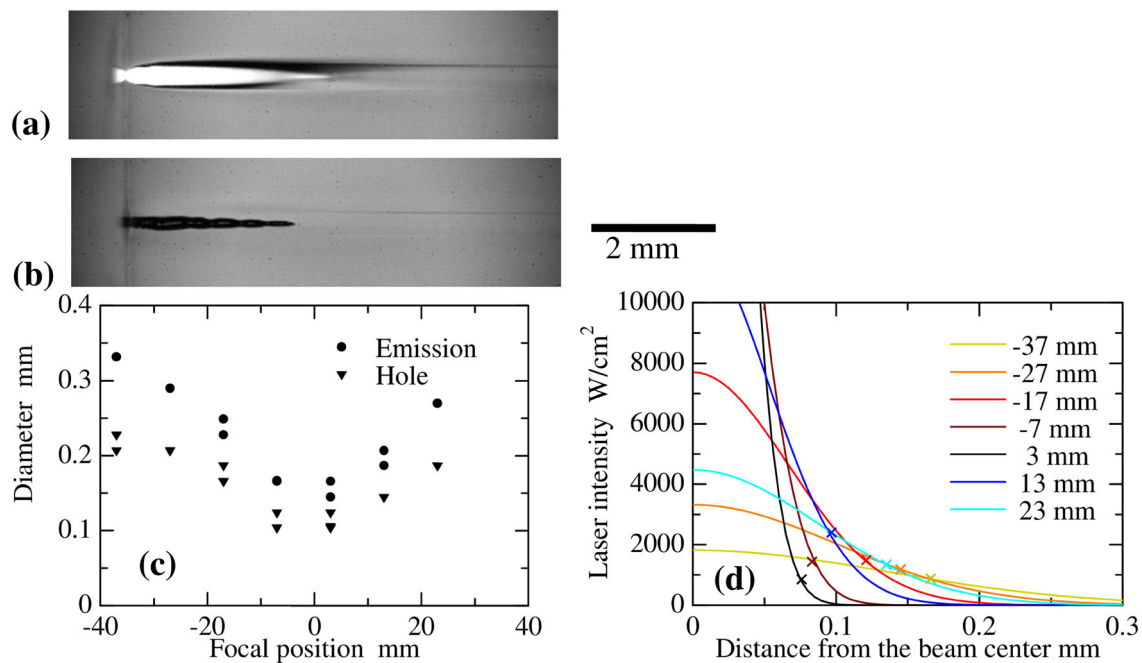


Fig. 5 Holes drilled using different defocus distances. Snapshots taken one frame before the ejection and of the drilled hole are shown in **a** and **b**, respectively. The laser power was 212 W, and the defocus distance was -37 mm. **c** The influence of the defocus distance on the

emission and hole diameters. **d** Laser intensity profiles at the glass surface. Illumination time was set at 0.7 s (where the defocus distance was set at -37 and $+23$ mm) and 0.5 s (where the defocus distance was set at -27 and $+13$ mm)

be degraded, and as a result, voids form with the free oxygen [13, 14]. The temperature at the light absorption point has been estimated to be >5000 K from the emission spectrum [11]. If we consider the fact that these voids formed in our experiments, then the glass temperature must have reached a higher level than the glass degradation temperature. The spindle-shaped emission is also under high pressure while the high-temperature area is confined within the glass. At the instant that the spindle-shaped emission forefront reaches the glass surface, the confined pressure is released, and the glass is both evaporated and degraded. Glass is ejected from the surface and the hole is drilled explosively. Therefore, the shapes of the drilled hole and the spindle-shaped emission were similar. If we consider the fact that the two voids near the bottom of the hole also moved and expanded, then similarly high-temperature and high-pressure conditions also existed in the vicinity of the hole.

Content equivalent to a cylinder with a diameter of ~ 110 μm and a depth of ~ 4 mm was ejected, and thus, the hole was drilled. The duration of the hole drilling process could not be observed accurately because of the spindle-shaped emission. However, the glass ejection from the surface is no longer observed after $+250$ μs , and the results thus indicate that the hole is drilled within 250 μs . Assuming that the glass that was located at a depth of 4 mm moved to the surface and was then ejected externally

within 250 μs , the average ejection speed is therefore >16 m/s.

The spindle-shaped emission propagation velocity increased proportionately with increasing laser power, as shown in Fig. 4f. This result corresponded well with the numerical calculation results shown in the literature [17] and with the fiber fuse results [19, 20]. The relationship between the spindle-shaped emission propagation velocity and the lengths of both the spindle-shaped emission and the hole was plotted in Fig. 4g and was shown to be in proportion. The reason for this relationship is considered as follows. In the numerical calculation results in [17], the laser beam propagating in the glass was absorbed within 30 μm of the forefront of the emission. The laser beam did not reach the other side of the glass because of this absorption, and the temperature decreased because of thermal conduction. Consider the temperature change at a point on the optical axis, when the emission was detected by the camera, the temperature increased rapidly because of the absorption of the passing light and then decreased by thermal conduction. After a certain time, the temperature decreased and emission was no longer detected. It is supposed that the time domain temperature change and the threshold temperature for emission detection by the camera are constant, even when different laser powers are used. The emission length is in proportion to the emission

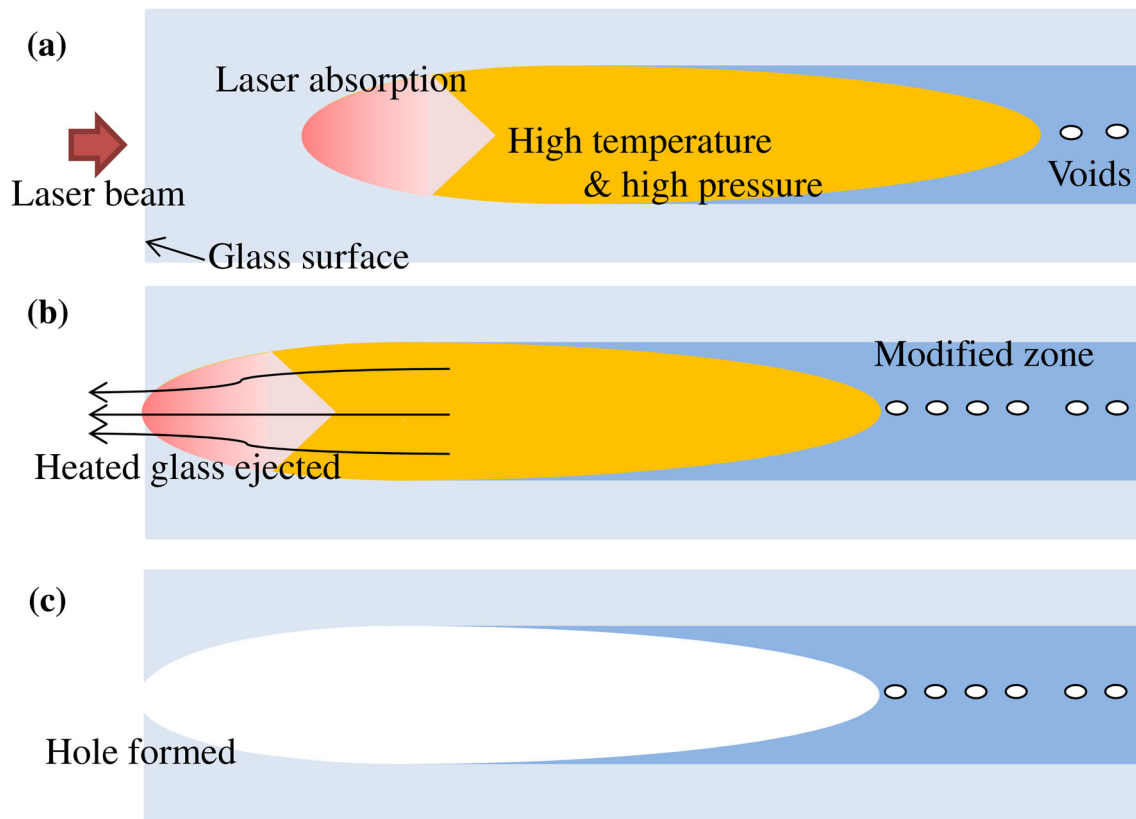


Fig. 6 Illustration of the hole formation process

propagation velocity. This supposition matched the results shown in Fig. 4g well.

The modification observed along the spindle-shaped emission trajectory was a concentric double-layered structure. Boundary layers caused by the inner and outer modification layers are indicated by arrows in Fig. 3b. The inner and outer modification diameters were ~ 120 and ~ 170 μm , respectively. The reason for the formation of these modifications is proposed as follows. Rapid heating and quenching of the glass under laser illumination causes increments in the fictive temperature and density of the glass. The density increment in turn causes a change in the refractive index of the glass. Because the density increment in the inner modification of the glass causes a volume decrement, tensile stress is therefore applied in the surrounding area. This tensile-stressed region is observed as the outer modification zone [16]. The boundary lines of the double-layered structure are clearly observed on the absorbent side; however, in the hole-drilled region, the boundary lines are not clear. Figure 3 shows that the inner modification coincides with the drilled hole diameter of ~ 110 μm . In the area surrounding the drilled hole, the boundary line between the outer modification and the base material can barely be recognized. The reason for this disappearance of the outer modification was that the inner

material did not actually exist and the tensile stress is thus not applied in the surrounding area. In the double-layered structure, the decrement of the inner modification volume causes the tensile stress in the outer modification. However, this tensile stress is not applied in the area surrounding the hole, because the surface of the hole behaves as a free end. This result agrees with the results of a previous paper [16].

3.5 Application to a through-hole

As described above, the glass was drilled on the light source side, and the maximum length of the drilled hole was more than 5 mm. However, the absorbent side of the glass was cracked. Through-hole drilling was demonstrated as follows. Silica glasses with thicknesses of 10 and 3 mm were used as the initiation glass and the workpiece, respectively. Figure 7 shows the in situ observation results. The spindle-shaped emission that was generated in the initiation glass moved toward the light source in the same manner as that shown in Fig. 2. At the instant that the spindle-shaped emission reached the boundary surface between the initiation glass and the workpiece, i.e., at -5350 μs , the initiation glass cracked. However, the spindle-shaped emission progressed continuously into the

workpiece. The spindle-shaped emission behavior in the workpiece was same as that in the initiation glass. However, cracking was only observed in the initiation glass as an effect of passing through the boundary surface. At 0 μs , the spindle-shaped emission forefront reached the workpiece surface on the light source side. The glass was then ejected and the hole was thus drilled. The drilling process was same as the process in which the 10-mm-thick glass alone was used.

The initiation glass and the workpiece were lightly bonded together after the experiment. However, the bond was easily separated manually. Figure 8 shows the observed results for the workpiece that was peeled from the initiation glass. Figure 8a shows a microscopic image from the side surface. Figure 8b, c shows scanning electron microscope (SEM) images of the light source side surface, i.e., the ejection nozzle, and the boundary surface, i.e., the spindle-shaped emission entry, respectively. The fact that the drilled hole was a through-hole was verified using flowing liquid. Figure 8c shows that the spindle-shaped emission entry hole of the workpiece is roughly circular in shape and that an area surrounding the hole with a diameter

of 200 μm has split off and has become concave. When the spindle-shaped emission passes through the boundary surface between the initiation glass and the workpiece, the high temperature caused a fused junction. This fused junction area causes the concave region on the workpiece when the boundary is separated. Some cracks were also observed in the radial direction (as indicated by the arrows). The transverse transmitted observation (Fig. 8a) clarifies that the depths of these cracks (indicated by an arrow) were less than 100 μm .

Figure 8b shows that the area surrounding the ejection nozzle on the workpiece surface forms an embossment and that fine glass fibers fly off in the radial direction. Part of the molten glass that was ejected from the ejection nozzle adhered to the surface and formed the embossment. A through-hole was drilled in a glass with a thickness of 3 mm though there was slight crack in the neighboring region of the boundary. Because the hole diameter was $\sim 100 \mu\text{m}$, the aspect ratio was calculated to be ~ 30 , and the machining time was less than 0.5 s. A high-aspect-ratio hole was therefore successfully drilled using an inexpensive infrared CW laser in a short time.

4 Summary

We have demonstrated a novel method for drilling of silica glass using a CW laser. The CW-LBI phenomenon was used for the drilling method. Initially, the CW-LBI phenomenon occurred in bulk glass, and a spindle-shaped emission propagated toward the light source. When the forefront of the spindle-shaped emission reached the surface of the silica glass, the glass was ejected from the surface. The glass ejection process occurred for a time of $\sim 250 \mu\text{s}$. A hole with a diameter of $\sim 110 \mu\text{m}$ and length of $\sim 4 \text{ mm}$ was drilled.

The spindle-shaped emission and hole lengths increased linearly with increasing laser power in the range between 111 and 277 W. The maximum power was limited by the laser oscillator specification, and the CW-LBI phenomenon was not observed for laser powers of 89 W. The maximum hole length was more than 5 mm. The laser power dependence of the spindle-shaped emission propagation velocity is also linear, and the velocity increases with increasing laser power. The diameter of the holes varied with varying focus positions. The focus position was varied in the range from -47 to 37 mm , and at the focus positions of -47 and 37 mm , the CW-LBI phenomenon was not observed. The hole diameters were thinner at the focus position of $\sim 0 \text{ mm}$ and increased with increasing levels of defocusing.

Through-hole drilling was demonstrated by drilling of two stacked silica glass pieces. A through-hole was drilled

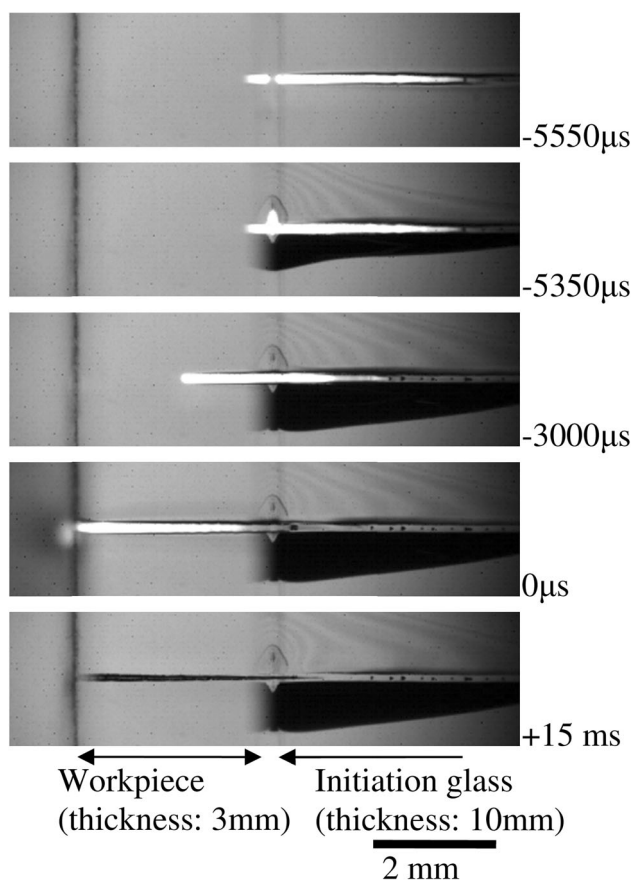


Fig. 7 Time-lapse photographs taken during emission propagation and hole formation using two glass pieces. The laser power was 212 W, and the defocus distance was -7 mm

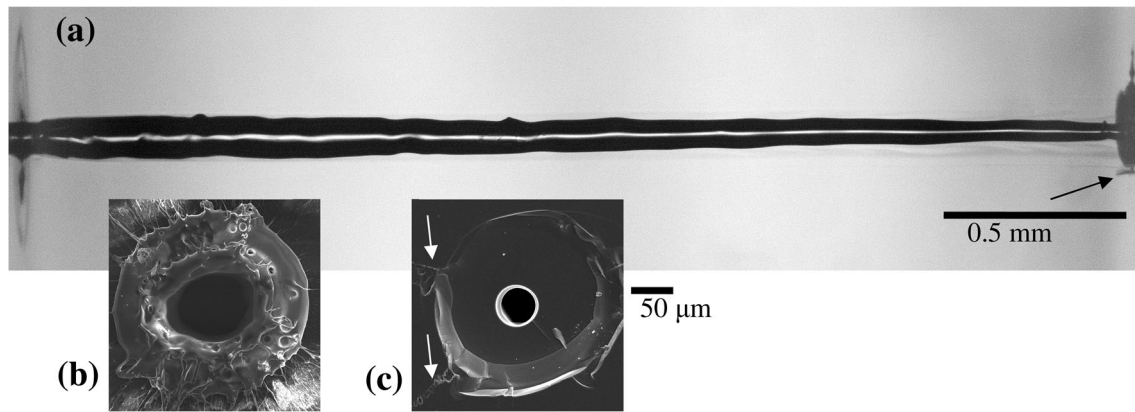


Fig. 8 Hole drilled through glass pieces with a total thickness of 3 mm. The transverse cross section is shown in **a**. SEM images around the hole on the laser-illuminated side and in contact with

another glass are shown in **b** and **c**, respectively. The laser power was 212 W, and the defocus distance was -7 mm

in a 3-mm-thick glass, although the neighboring region of the boundary with the initiation glass was slightly cracked. The aspect ratio was calculated to be ~ 30 .

Acknowledgments The loan of the laser oscillator from Fujikura Ltd. is gratefully acknowledged by the authors.

References

1. R.R. Gattass, E. Mazur, *Nat. Photonics* **2**, 219 (2008)
2. D. Esser, S. Rezaei, J. Li, P.R. Herman, J. Gottmann, *Opt. Express* **19**, 25632 (2011)
3. H. Varel, D. Ashkenasi, A. Rosenfeld, M. Wahmer, E.E.B. Campbell, *Appl. Phys. A* **65**, 367 (1997)
4. L. Shah, J. Tawney, M. Richardson, K. Richardson, *Appl. Surf. Sci.* **183**, 151 (2001)
5. S. Karimelahi, L. Abolghasemi, P.R. Herman, *Appl. Phys. A* **114**, 91 (2014)
6. H. Hidai, S. Matsusaka, A. Chiba, N. Morita, *Appl. Phys. A* **120**, 357 (2015)
7. Y. Matsuoka, *Appl. Phys. A* **88**, 319 (2007)
8. O. Hiroshi, Y. Yoshikazu, *Jpn. J. Appl. Phys.* **42**, 5R 2881 (2003)
9. D.J. Hwang, T.Y. Choi, C.P. Grigoropoulos, *Appl. Phys. A* **79**, 605 (2004)
10. Y. Li, K. Itoh, W. Watanabe, K. Yamada, D. Kuroda, J. Nishii, Y.Y. Jiang, *Opt. Lett.* **26**, 1912 (2001)
11. E.M. Dianov, V.E. Fortov, I.A. Bufetov, V.P. Efremov, A.E. Rakitin, M.A. Melkumov, M.I. Kulish, A.A. Frolov, *IEEE Photonics Tech. Lett.* **18**, 752 (2006)
12. S. Todoroki, *Fiber Fuse: Light-Induced Continuous Breakdown of Silica Glass Optical Fiber* (Springer, Berlin, 2014)
13. S.I. Yakovlenko, *Laser Phys.* **16**, 1273 (2006)
14. H.L. Schick, *Chem. Rev.* **60**, 331 (1960)
15. H. Hidai, M. Yoshioka, K. Hiromatsu, H. Tokura, *Appl. Phys. A* **96**, 869 (2009)
16. H. Hidai, M. Yoshioka, K. Hiromatsu, H. Tokura, *J. Am. Ceram. Soc.* **93**, 1597 (2010)
17. S. Itoh, H. Hidai, H. Tokura, *Appl. Phys. A* **112**, 1043 (2013)
18. D. Baeuerle, *Laser Processing and Chemistry*, 3rd edn. (Springer, New York, 2000), p. 81
19. R.I. Golyatina, A.N. Tkachev, S.I. Yakovlenko, *Laser Phys.* **14**, 1429 (2004)
20. S. Todoroki, *Optical Fiber Communication Conference and Exposition and the National Fiber Optic Engineers Conference (OFC/NFOEC)*, JW2A.11 (2013)